Nano- to Macro-Sized Heterogeneities Using Cleavable Diblock Copolymers

James T. Goldbach,† Kristopher A. Lavery, Jacques Penelle,‡ and Thomas P. Russell*

Department of Polymer Science and Engineering, University of Massachusetts at Amherst, Amherst, Massachusetts 01003-4530

Received June 2, 2004; Revised Manuscript Received September 20, 2004

ABSTRACT: Polystyrene-*block*-poly(methyl methacrylate) copolymers containing [4π + 4π] anthracene photodimer at the junction point between the blocks (PS-AA-PMMA) can be cleaved to the parent homopolymer blocks upon heating above 130 °C or by UV irradiation at 280 nm. PS-AA-PMMA was characterized and then used in thin films to create micro- to macroscale poly(methyl methacrylate) (PMMA) domains in a polystyrene (PS) matrix. Microphase-separated morphologies in thin films were initially achieved by annealing spin-coated films in supercritical carbon dioxide at 80 °C. Subsequent heating and/or UV irradiation was used to cleave the copolymer junction point, affecting an in situ conversion of the diblock copolymer to its parent homopolymers. The evolution of phase separation, from microdomains of PMMA in a matrix of PS to macrophase-separated structures, was investigated by SFM. Subsequent washing with selective solvents removed homopolymer, producing raised nanostructures or nanoporous templates.

Introduction

Recently, there has been much interest in the control of the size of features on surfaces in the range of tens to hundreds of nanometers. Precise control of the sizes of moieties in this range is needed in technological areas ranging from data storage media, to optoelectronics, to separation science. In particular, diblock copolymer films,[1−7] blends of homopolymers,[8−16] and homopolymer/block copolymer mixtures[17−28] have attracted much attention due to their interesting phase behavior, potential use as commercial materials, and ability to control domain sizes.

Diblock copolymers microphase separate into well-defined, uniform morphologies that range in size from ∼10 to ∼100 nm. Changing the molecular weight of the two polymer blocks changes the shape and size of these domains.[29] In addition, the orientation of microdomains can be controlled by the use of external fields, which has been the subject of intense study lately.[1,2,5,6,30−35] The size of the microstructures obtained with block copolymers is limited by the molecular weight. However, as molecular weight is increased to increase the size of structures, the kinetics of orientation of the microdomains is slow, often trapping the copolymer in a nonequilibrium state, leading to a practical limit of ∼50 nm in domain size.[7] To circumvent this limit, phase-separated blends of homopolymer and diblock copolymer have been used. The diblock copolymer stabilizes polymer−polymer interfaces, reducing the interfacial energy penalty between homopolymer domains, and allows for the production of domains larger than ∼100 nm depending on the ratio and nature of the diblock copolymer to homopolymer.[17−21,25−26,28,36−38]

When the ratio of homopolymer to diblock copolymer is low, microphase separation occurs and the homopolymer segregates into one of the microdomains, increasing its volume. As the concentration is increased, the microdomains swell to accommodate the additional homopolymer and a change in morphology can result. If the ratio of homopolymer to diblock is high, macrophase separation will occur and the size of structures will be determined by the relative amounts of the components. In all of these cases the ratio of diblock copolymer to homopolymer is predetermined before casting of the film and the domain size is relatively uniform throughout the sample.

Here, a method is shown by which diblock copolymer/homopolymer blends can be produced in situ in thin films by converting the diblock copolymer to its parent homopolymers. This can be achieved by the application of heat or UV irradiation at a specific wavelength where the junction point between the blocks is cleaved. Upon annealing or washing with solvents selective for either block, various domain sizes and morphologies were produced in thin films and investigated by scanning force microscopy (SFM).

Experimental Section

Materials. The diblock copolymer investigated in this study was a ∼70 k poly(styrene-*block*-methyl methacrylate) asymmetric (70:30 v/v) copolymer with an anthracene [4π + 4π] photodimer at the junction point between the blocks (PS-AA-PMMA). PS-AA-PMMA was synthesized as described previously, and its structure is outlined in Scheme 1.[39] Benzyl alcohol end-functionalized random copolymer of styrene and methyl methacrylate (PS-*r*-PMMA) (58 mol % styrene) was synthesized by nitroxide-mediated controlled free-radical polymerization as described previously.[40]

General Procedures and Instrumentation. Silicon wafers (100) were purchased from International Wafer Source, immersed in a Nochromix sulfuric acid bath for 24 h, rinsed with deionized water for 4 h, and dried under a flow of nitrogen. Thermal cleavage studies in thin films were carried out using a VWR brand, model 400 temperature-controlled hot

* To whom correspondence should be addressed.
† Current address: ATOFINA Chemicals Inc., 900 First Ave., King of Prussia, PA 19406. E-mail: james.goldbach@atofina.com.
‡ Current address: Laboratoire de Recherche sur les Polymères (LRP), Université Paris 12−CNRS, 2-8 rue H. Dunant, F-94320 Thiais, France. E-mail: penelle@glvt-cnrs.fr.

10.1021/ma0489117 CCC: $27.50
Published on Web 11/16/2004

Scheme 1. Representation of the PS-AA-PMMA Asymmetric Diblock Copolymer, Illustrating the Anthracene Photodimer Junction Point, before and after Thermal or UV Cleavage

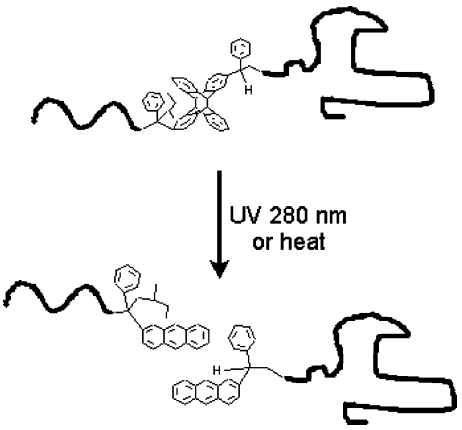

plate in air. UV cleavage studies were performed using a using a short-wave 400 W mercury lamp (UV Products, Inc., model XX-15S) and a UV band-pass filter with transmittance maximum at 280 nm (Cheshire Optical, Swanzey, NH, model 280.0 IF 12). UV intensity at 280 nm was 0.31 $mW \cdot cm^{-2}$, as measured at the sample surface. SFM images were obtained using a Digital Instruments Dimension 3000 scanning force microscope in tapping mode with etched silicon tips (Nanoprobe). The spring constant of the tips was 40−66 $N \cdot m^{-1}$, as specified by the manufacturer. Film thicknesses were measured at a 70° incidence angle by ellipsometry using a Rudolph Research AutoEl-II Ellipsometer equipped with a helium−neon laser. Size exclusion chromatography (SEC) was performed on an in-house built system using WinGPC data collection software, three-column set (Polymer Labs, Inc., 2 Mixed-D, and 1 50 Å, 5μm 300 × 7.5 mm), variable wavelength UV (Waters 486), and refractive index (Wyatt Optilab DSP) detector. The system was calibrated with respect to PS and PMMA standards (Polymer Labs, Inc.). Peak deconvolutions and curve fitting were done using Galactic Industries Corp., GRAMS/32 software, version 4.14.

Kinetics study of the Thermal Cleavage of PS-AA-PMMA. A 0.030 g amount of PS-AA-PMMA was dissolved in 0.50 mL of toluene, filtered, poured on a glass slide, and allowed to air dry for 24 h. This film was then heated at 170 °C in air, periodically removing samples for analysis by SEC.

S**tudy of the UV Cleavage of PS-AA-PMMA.** A second film was prepared as described in the previous section. This sample was irradiated for 88 h at an intensity of 0.31 $mW \cdot cm^{-2}$, wavelength of 280.0 ± 5.0 nm, using a 280.0 nm band-pass filter under vacuum. Samples were taken periodically for analysis by SEC.

Surface Modification/Thin Film Preparation. Surfaces with balanced interfacial interactions were prepared by spin coating a 3.0 wt % solution of benzyl alcohol end-functionalized polystyrene-*ran*-poly(methyl methacrylate) with 58 mol % styrene (PS-*r*-PMMA)[40] in toluene at 1500 rpm onto a clean silicon wafer. After annealing at 170 °C for 3 days under vacuum, the substrates were rinsed with toluene and dried under nitrogen flow. Passivated silicon surfaces were prepared by immersing a clean silicon wafer in a 5% aqueous solution of hydrofluoric acid for 3 min. They were then rinsed with deionized water for 15 min and dried under a flow of nitrogen. Silicon oxide surfaces were prepared by rinsing a clean silicon wafer with filtered toluene and then drying under nitrogen. Thin films of PS-AA-PMMA were prepared on the aforementioned substrates by spin coating a 1.0 wt % solution of copolymer in toluene at 2800 rpm. Thin film annealing under supercritical fluid carbon dioxide (SCF CO_2) was performed at 80 °C and 2000 psi for 72 h using an in-house built, cold wall, high-pressure vessel (Grayloc Products) with carbon dioxide supplied using a high-pressure ISCO syringe pump.

Results and Discussion

Methodology for Studying the Thermal Cleavage of PS-AA-PMMA to Its Parent Homopolymer Blocks. It is known that the [4π + 4π] photodimer of anthracene will rapidly revert to the parent anthracenes at temperatures greater than 180 °C.[41] The thermal properties of our PS-AA-PMMA were investigated by monitoring the selective degradation of the diblock copolymer to its parent homopolymer blocks upon heating a bulk sample at 170 °C for varying times. At this temperature thermal cleavage of the anthracene photodimer is sufficiently slow to provide a convenient time scale for which to take samples for analysis by SEC.

SEC with UV detection set at an absorbance of 254 nm was used to monitor the reaction. At this wavelength both the phenyl side groups and anthracene end groups absorb UV radiation. As a result, the detector responds to the absorbance of the phenyl groups in the PS block in the PS-AA-PMMA diblock copolymer, the cleaved PS-A homopolymer (PS absorbance + anthracene end-group absorbance), the anthracene end group of the PMMA-A cleaved homopolymer, as well as a higher molecular weight impurity (low elution volume shoulder) that arises from the end photocoupling synthetic methodology.[39] As the heating time was increased, a decrease in the peak corresponding to the PS-AA-PMMA was observed in addition to the appearance of a peak at the elution volume expected for the PS-A as well as a peak at longer elution volumes corresponding to the PMMA-A homopolymer. The overlapping peaks were deconvoluted, and Gaussian/Lorentzian mixed curves were fit to these deconvoluted peaks.

The ratio of the area of the deconvoluted curves corresponding to the parent diblock and cleaved PS block in the SEC chromatograms were compared directly after correcting for absorbance of anthracene end group on the PS. At 254 nm the PMMA block does not absorb UV radiation, so the signal from the UV detector corresponds only to anthracene end groups. To correct for the absorbance from the anthracene end groups on the PS-A, the area calculated from the PMMA-A peak was subtracted from that of the PS-A peak. Figure 1a shows a representative SEC trace (solid line) with deconvoluted peaks (dashed line) for PS-AA-PMMA heated at 170 °C for 60 min. The ratio of the deconvoluted, corrected peak for PS-A was compared to the total (PS-A + PS-AA-PMMA) to obtain the percent cleaved over time (Figure 1b). Using this same methodology, results for the photoinduced cleavage were also obtained.

Results for the Thermal Cleavage of PS-AA-PMMA to Its Parent Homopolymer Blocks. The linear plot of the natural logarithm of the ratio of the measured (A) versus the initial absorbance (A_o) ($\ln(A/A_o)$) versus time obtained from the results included in Figure 1b (T = 170 °C) showed first-order kinetics (Figure 1c). A value for the dissociation rate constant of 1.070×10^{-4} $L(mol \cdot s)^{-1}$ was obtained from the slope of the regression line. This value is of the same order of magnitude as the literature value of 1.721×10^{-4} $L(mol \cdot s)^{-1}$ for anthracene photodimers of low molecular weight containing alkyl substituents on the 9-position of the parent anthracene.[41] It is known that adding substituents to anthracene photodimers can change the photodissociation rate constant by orders of magnitude, so this suggests that the photodissociation of the junction point is not greatly affected by the attachment of

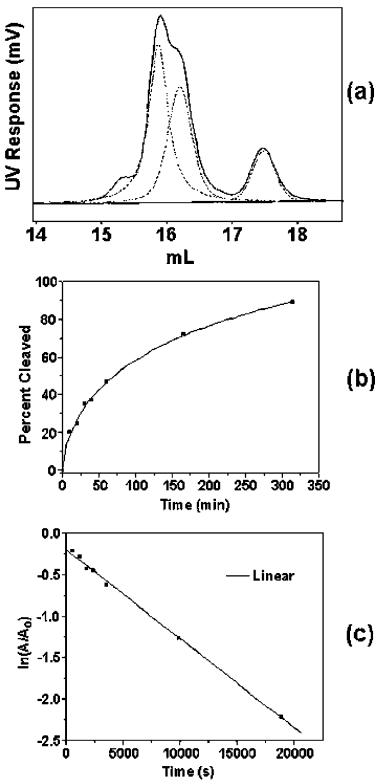

Figure 1. (a) Representative SEC chromatogram showing peaks for PS-AA-PMMA, PS homopolymer, and PMMA-A after thermal cleavage. Dashed lines: peak fits. (b) Plot of percent of diblock cleaved versus time. (c) Linear kinetics plot of cleavage data from calculation of areas under peak fits.

relatively large polymer chains to the photodimer. It should be noted that a linear fit to the data in the kinetic plot does not pass through the origin, suggesting that initially some additional degradation occurs at the early times. This may be due to a small amount of head-to-head photodimers present in the system. Head-to-head photodimers are known to be more thermally unstable than their head-to-tail analogues,[41,42] which could contribute to the observed initial deviation.

UV Cleavage of PS-AA-PMMA to Its Parent Homopolymer Blocks. In addition to reverting to its parent anthracenes upon heating, the anthracene photodimers are also known to cleave upon UV irradiation at an appropriate wavelength. For our system irradiation at 280 nm is sufficient to afford the photodimer cleavage.[41,43,44] Additionally, PS and PMMA have negligible absorbances at this wavelength; thus, there is no possible degradation or cross-linking of the polymeric portions of the system.

As in the study of the thermal cleavage, SEC with UV detection at 254 nm was used to monitor the cleavage reaction. The peaks were deconvoluted, fit, and corrected in the same fashion as before. Figure 2a shows a representative SEC chromatogram of the polymer after irradiation of a thick film (~5 μm) for 4 h. Peaks corresponding to the PS and PMMA homopolymer blocks are clearly visible as well as a peak for remaining PS-AA-PMMA. The kinetic plot (percent of dissociation versus time) (Figure 2b) indicates that greater than 70% cleavage of the diblock can be achieved, except that the reaction becomes very slow after 60−65% cleavage. A likely explanation for this observation is the presence of side reaction anthracene dimers during irradiation, such as reaction with adventitious oxygen, producing a

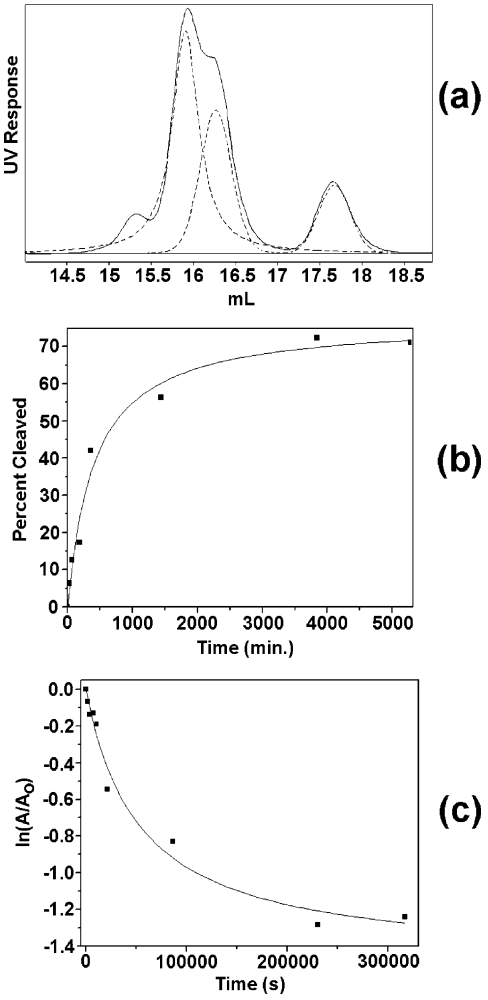

Figure 2. (a) SEC chromatogram of UV-irradiated PS-AA-PMMA after 4 h of irradiation. Dashed line: Gaussian peak fits. (b) Plot of percent of diblock cleaved versus time. (c) Kinetics plot of cleavage data from calculation of areas under peak fits. Solid line: hyperbolic curve fit drawn as support to the eye.

noncleavable moiety. The relative concentration of anthracene dimer units is very small, so even a low concentration of oxygen would interfere with the UV cleavage reaction. Another potential explanation could be the presence of a competition for the photons by the newly formed anthracene end groups with equilibrium being established between photon absorption and photodimer cleavage or perhaps by competition for photons by the total absorption of the material. The molar absorptivity of PS at 280 nm was measured by UV−vis absorption spectroscopy and found to be very low, ~230 L·(mol·cm)$^{-1}$, as expected, so it is unlikely that absorption by PS is a major factor in the reduction of the rate of UV cleavage.

Supercritical Fluid (SCF) CO_2 Annealing of PS-AA-PMMA Thin Films. To obtain a microphase-separated morphology in PS-*b*-PMMA thin films, it is necessary to impart mobility to the polymer chains so they can reach their equilibrium morphology. This is typically accomplished by heating the bulk polymer above the glass-transition temperature (T_g) or by introduction of a solvent or plasticizer to decrease the T_g. In the case of PS-AA-PMMA films, temperatures above 150 °C are needed to provide sufficient polymer mobility and degradation of the anthracene photodimers will occur.

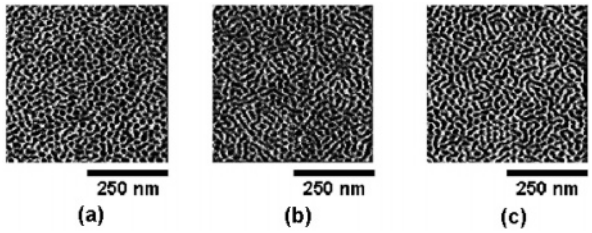

Figure 3. SFM phase images of ~30 nm thick PS-AA-PMMA thin films after annealing in SCF CO_2. (a) Thin film on neutral brush substrate. (b) Thin film on passivated silicon. (c) Thin film on silicon oxide.

SCF CO_2 is known to dramatically depress the glass-transition temperature of PS and PMMA.[45−49] A 1.0% solution of PS-AA-PMMA was spin coated onto neutral brush modified, passivated, and silicon oxide substrates and then annealed at 80 °C under SCF CO_2 for 72 h. This treatment allowed sufficient mobility for the copolymers to reach their equilibrium morphology without thermal degradation. After 72 h the SCF CO_2 cell was cooled and rapidly vented. Figure 3 shows SFM phase images of the resulting films.

The phase response from the SFM for the images depicted in Figure 3 is inverted relative to a thermally annealed PS-*b*-PMMA copolymer thin film. The PMMA domains typically give higher response (brighter) than that of the PS domains due to the higher modulus of PMMA versus PS.[7,50,51] In these samples, however, the matrix (PS) exhibited a higher phase response than the minor component (PMMA). It is known that under SCF CO_2 conditions PMMA swells by 15% in SCF CO_2 whereas PS swells by ~10%,[49] Thus, the PMMA domains occupy more volume relative to PS than in a non-SCF CO_2-swollen state. When the pressure is vented the PMMA domains relax into a volume larger than they would normally occupy, resulting in a slight depression, which is viewed in the SFM phase image as an area of lower apparent modulus (darker) (Figure 3). It should also be noted that despite the differential dilation, the morphology comprised of PMMA cylindrical microdomains is maintained.

It can be seen that interfacial interactions have been mediated. On a neutral brush surface one would expect the microdomains to be oriented normal to the surface end on a silicon oxide surface; the microdomains would be expected to orient parallel to the surface.[1,7,50,51] Neither preferred orientation is seen. Consequently, the SCF CO_2 must mediate interface interactions. Though control of microdomain orientation was lost, SCF CO_2 annealing afforded a microphase-separated morphology starting point with no degradation of the PS-AA-PMMA.

Monitoring Thin Film Morphology Upon Additional Heating. In the previous sections we determined that PS-AA-PMMA gradually cleaves to its parent homopolymers over approximately 4 h upon heating at 170 °C. As the homopolymer ratio was increased upon additional heating at 170 °C, changes in morphology in thin films were monitored by SFM. Figure 4 shows six representative SFM phase images of a SCF CO_2 annealed, 30 nm thick, PS-AA-PMMA film on a neutral brush substrate that was heated in air for increasing periods of time. In Figure 4a the film was heated for 1 min at 170 °C, and the SFM phase image has inverted to higher response for the PMMA domains due to the relaxation of the film to its non SCF CO_2-swollen equilibrium state. Over time at 170 °C microphase-separated structures increase in size to accommodate the increasing fraction of homopolymer being generated in the system (Figure 4b and c). Upon extended heating (Figure 4d), large domains of homopolymer become visible. These domains increase in size (Figure 4e) until the entire surface becomes saturated with PS homopolymer. From the SFM height images (not shown) we can obtain the root-mean-square film roughness. This roughness gradually increases, goes through a maximum, and then decreases as the polystyrene covers the air interface (Figure 5).

Film Morphology after Heating at 170 °C and Subsequent Washing with Cyclohexane. To investigate the morphology beneath the surface-segregated PS, microphase-separated films were annealed for predetermined amounts of time and then washed for 5 min with cyclohexane to remove the PS homopolymer. This

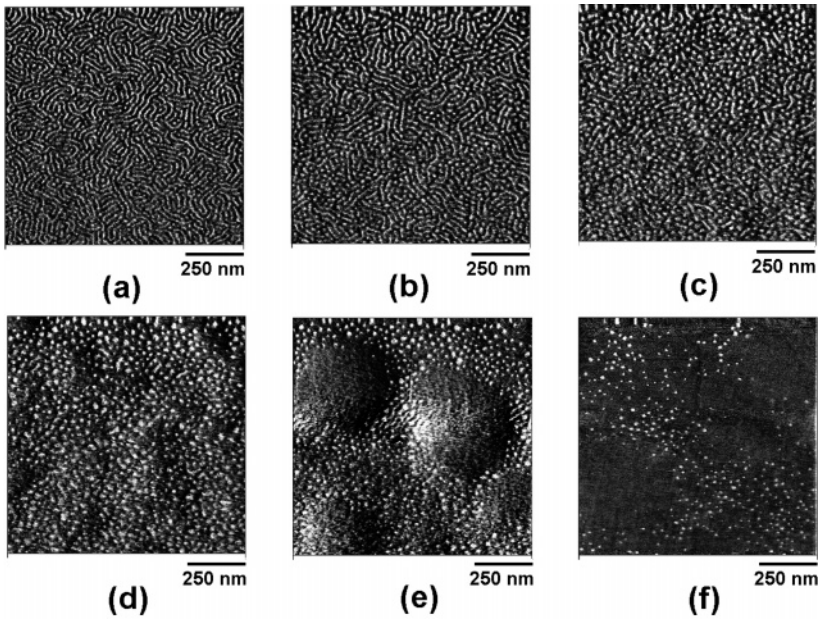

Figure 4. SFM phase images of ~30 nm thick PS-AA-PMMA thin films after annealing in SCF CO_2 with subsequent heating at 170 °C for (a) 1, (b) 7.5, (c) 20, (d) 40, (e) 80, and (f) 120 min.

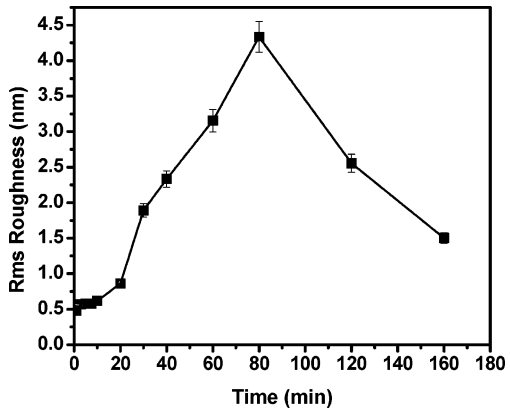

Figure 5. Plot of root-mean-square film roughness versus heating time calculated from films annealed in SCF CO_2 then heated at 170 °C.

treatment removed surface-segregated PS homopolymer as well as any PS remaining in the matrix phase of the PS-AA-PMMA. Figure 6 shows the underlying morphology for varying heating times before and after cyclohexane washing. Figure 6a shows the SFM height and phase images of the initial, SCF CO_2-annealed film. Upon heating at 170 °C a change in morphology is observed where, as before, the PMMA microdomains become visible and slightly raised. Subsequent cyclohexane washing removes PS and the PMMA microdomains become slightly more pronounced (Figure 6b) but retain the structure similar to the initial film.

When the initial film is heated for 5 min, a change in morphology to more cylindrical or rounded structures is observed. These structures seem to be partially covered by PS, and film has very low roughness. After washing with cyclohexane, however, a marked increase in film roughness is observed and PMMA structures appear as rounded 'mushrooms' above the level of the PS matrix (Figure 6c). After cyclohexane washing, the PMMA structures now protrude (~5 nm) above the top of the film, producing more rounded, mushroom-type, structures. A diagram of this structure formation is shown in Scheme 2. Similarly, when the initial film is

Scheme 2. (Left) Representation of PMMA 'Mushroom' Formation after PS Homopolymer Removal. (a) Washing with Cyclohexane Removes PS, (b) Remaining PMMA Microdomains Rapidly Relax To Form 'Mushroom-Cap'-Type Morphologies on the Surface of the Film. (Right) Representation of 'Nanohole' Formation after Washing with Acetic Acid Removes PMMA. (c) Annealing at 170 °C Causes PS Homopolymer to Segregate to the Air Interface, (d) Acetic Acid Washing Removes PMMA Homopolymer

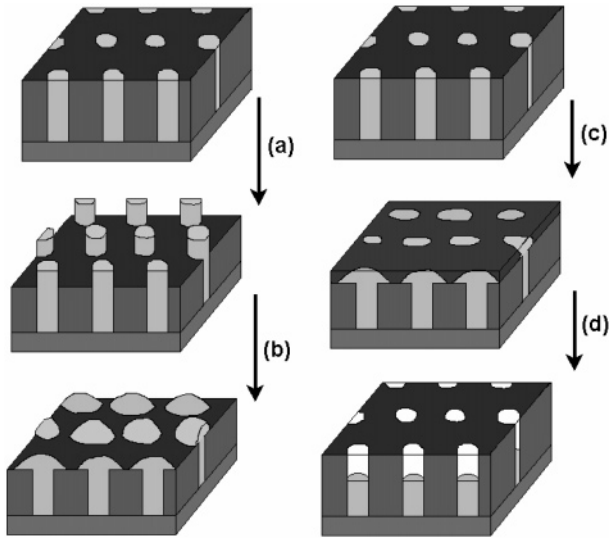

heated for 15 min, the same behavior is observed; however, the density of PMMA structures per area is reduced, even though the average diameter of the structures remains relatively constant. Again, cyclohexane washing causes the PMMA structures to become more pronounced (Figure 6d). The average period of the structures was calculated by taking the Fourier transform of the SFM images. An increase in average center-to-center distance between structures is observed as heating time is increased. In addition, the average film roughness increases, goes through a maximum, and then decreases as the density of structures per area decreases while the average structure diameter increases from ~45 nm for Figure 6a and b to ~60 nm for

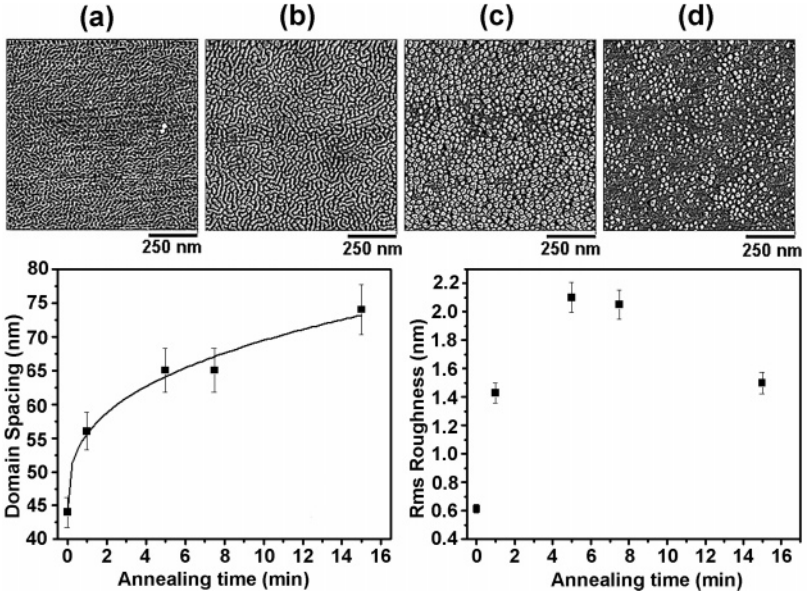

Figure 6. SFM phase images of ~30 nm thick PS-AA-PMMA thin films after annealing in SCF CO_2, heated at 170 °C for varying times, then washed with cyclohexane: (a) Initial film (no heating), (b) 170 °C for 2 min, cyclohexane washed, (c) 170 °C for 7.5 min, cyclohexane washed, (d) 170 °C for 15 min, cyclohexane washed.

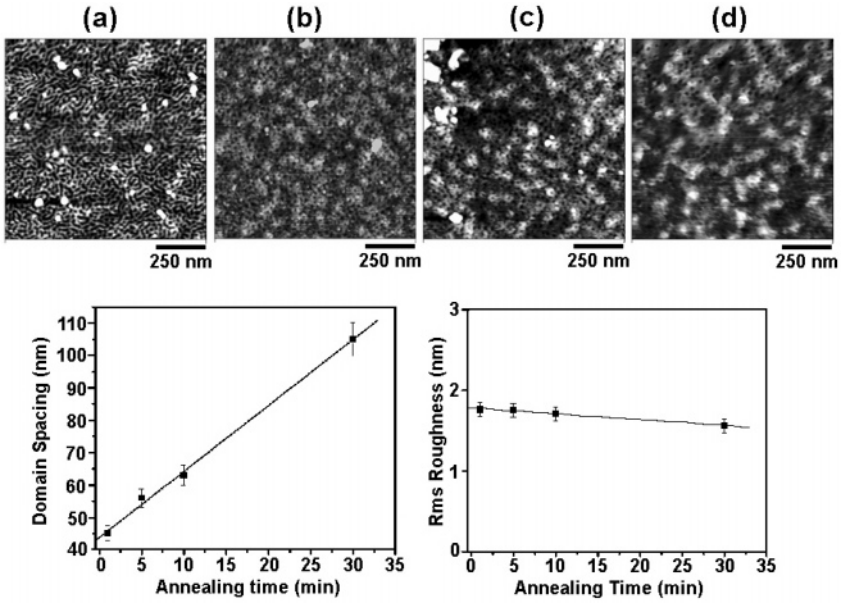

Figure 7. SFM height images of ~30 nm thick PS-AA-PMMA thin films after annealing in SCF CO_2, heated at 170 °C for varying times, then washed with acetic acid: (a) 170 °C for 1 min, acetic acid washed, (b) 170 °C for 5 min, acetic acid washed, (c) 170 °C for 10 min, acetic acid washed, (d) 170 °C for 30 min, acetic acid washed.

Figure 6c and d. This indicates a change in the overall morphology as the relative concentration of homopolymer is increased in the system. For low fractions of homopolymer, the original microstructure size and period is maintained, but as homopolymer content is increased, there is a jump in microstructure size and period. In this fashion, the areal density of PMMA structures can be controlled simply heating the microphase-separated film with subsequent washing of the film with cyclohexane.

Film Morphology after Heating at 170 °C and Subsequent Washing with Acetic Acid. An experiment similar to that outlined in the previous section was concurrently performed where the microphase-separated PS-AA-PMMA films were heated for varying lengths of time and then washed with acetic acid, a solvent selective for PMMA homopolymer. As before, an increase in the phase response of the PMMA microdomains at short heating times was observed followed by a change in morphology to more rounded, cylindrical-type structures. As in the previous samples, heating the microphase-separated films produced round or cylindrical domains of PMMA in the PS matrix (Figure 4). When these films were washed with acetic acid, the PMMA homopolymer was removed, leaving behind films with pores on the surface (Figure 7a−d). Increasing heating time decreased the areal density of structures as before, while their diameter remained relatively constant (~47 nm). This suggests that the PMMA microdomains are maintained as cylinders within the PS matrix film and are not simply dewetted PMMA domains on top of a contiguous PS film. In this fashion a PS film with varying areal density (porosity) of nanoholes can be produced, again simply by heating and washing a microphase-separated PS-AA-PMMA film.

Conclusions

The UV, thermal, and thin film morphology characteristics of PS-AA-PMMA diblock copolymer were characterized by SEC and SFM. This copolymer was shown to cleave to its parent homopolymer blocks upon heating at 170 °C or by UV irradiation at 280 nm. Thin films (~30 nm) were annealed in SCF CO_2 to obtain microphase-separated structure without significant degradation of the copolymer. These microphase-separated films were subsequently treated thermally to cleave the diblock to homopolymers. The resultant morphology and domain size can be controlled by varying the heating time. Heating and washing with selective solvent produces films that contain either round PMMA features on the surface or holes in a PS matrix, the areal density of which can be controlled by varying the heating times.

Acknowledgment. Financial support by a NSF grant (CTS-9871782), the NSF Partnership in Nanotechnology (DMR-9809365), and the University of Massachusetts Materials Research Science and Engineering Center (UMass-MRSEC) (DMR-8909365 and DMR-0213695) is gratefully acknowledged.

References and Notes

(1) Huang, E.; Pruzinsky, S.; Russell, T. P.; Mays, J.; Hawker, C. J. *Macromolecules* **1999**, *32*, 5299−5303.
(2) Huang, E.; Rockford, L.; Russell, T. P.; Hawker, C. J. *Nature* **1998**, *395*, 757−758.
(3) Liu, Y.; Russell, T. P.; Samant, M. G.; Stöhr, J.; Brown, H. R.; Cossy-Favre, A.; Diaz, J. *Macromolecules* **1997**, *30*, 7768−7771.
(4) Mansky, P.; DeRouchey, J.; Russell, T. P.; Mays, J.; Pitsikalis, M.; Morkved, T.; Jaeger, H. *Macromolecules* **1998**, *31*, 4399−4401.
(5) Mansky, P.; Russell, T. P.; Hawker, C. J.; Pitsikalis, M.; Mays, J. *Macromolecules* **1997**, *30*, 6810−6813.
(6) Mansky, P.; Liu, Y.; Huang, E.; Russell, T. P.; Hawker, C. *Science* **1997**, *275*, 1458−1460.
(7) Xu, T.; DeRouchey, J.; Seney, C.; Levesque, C.; Martin, P.; Stafford, C. M.; Russell, T. P. *Polymer* **2001**, *42*, 9091−9095.
(8) Kumar, S. K.; Russell, T. P. *Macromolecules* **1991**, *24*, 3816−3820.
(9) Ermi, B. D.; Karim, A.; Douglas, J. F. *J. Polym. Sci., Part B: Polym. Phys.* **1997**, *36*, 191−200.
(10) Sung, L.; Karim, A.; Douglas, J. F.; Han, C. C. *Phys. Rev. Lett.* **1996**, *76*, 4368−4371.
(11) Bruder, F.; Brenn, R. *Phys. Rev. Lett.* **1992**, *69*, 624−627.
(12) Steiner, U.; Klein, J.; Fetters, L. J. *Phys. Rev. Lett.* **1994**, *72*, 1498−1501.
(13) Krausch, G.; Dai, C.-A.; Kramer, E. J.; Marko, J. F. *Macromolecules* **1993**, *26*, 5566−5571.

(14) Karim, A.; Douglas, J. F.; Lee, B. P.; Glotzer, S. C.; Rogers, J. A.; Jackman, R. J.; Amis, E. J.; Whitesides, G. M. *Phys. Rev. E* **1998**, *57*, R6273−R6276.
(15) Krausch, G.; Kramer, E. J.; Rafailovich, M. H.; Sokolov, J. *Appl. Phys. Lett.* **1994**, *64*, 2655−2657.
(16) Jones, R. A. L.; Norton, L. J.; Kramer, E. J.; Bates, F. S.; Wiltzius, P. *Phys. Rev. Lett.* **1991**, *66*, 1326−1329.
(17) Winey, K. I.; Thomas, E. L.; Fetters, L. J. *Macromolecules* **1992**, *25*, 2645−2650.
(18) Spontak, R. J.; Fung, J. C.; Braunfeld, M. B.; Sedat, J. W.; Agard, D. A.; Kane, L.; Smith, S. D.; Satkowski, M. M.; Ashraf, A.; Hajduk, D. A.; Gruner, S. M. *Macromolecules* **1996**, *29*, 4494−4507.
(19) Bates, F. S.; Maurer, W.; Lodge, T. P.; Schulz, M. F.; Matsen, M. W.; Almdal, K.; Mortensen, K. *Phys. Rev. Lett.* **1995**, *75*, 4429−4432.
(20) Likhtman, A. E.; Semenov, A. N. *Macromolecules* **1997**, *30*, 7273−7278.
(21) Maurer, W. W.; Bates, F. S.; Lodge, T. P.; Almdal, K.; Mortensen, K.; Fredrickson, G. H. *J. Chem. Phys.* **1998**, *108*, 2989−3000.
(22) Schwahn, D.; Mortensen, K.; Frielinghaus, H.; Almdal, K. *Phys. Rev. Lett.* **1999**, *82*, 5056−5059.
(23) Frielinghaus, H.; Mortensen, K.; Almdal, K. *Macromol. Symp.* **2000**, *149*, 63−67.
(24) Frielinghaus, H.; Mortensen, K.; Almdal, K. *Physica B* **2000**, *276*, 375−376.
(25) Bodycomb, J.; Yamaguchi, D.; Hashimoto, T. *Macromolecules* **2000**, *33*, 5187−5197.
(26) Lee, J. H.; Balsara, N. P.; Chakraborty, A. K.; Krishnamoorti, R.; Hammouda, B. *Macromolecules* **2002**, *35*, 7748−7757.
(27) Vaidya, N. Y.; Han, C. D. *Polymer* **2002**, *43*, 3047−3059.
(28) Green, P. F.; Limary, R. *Adv. Colloid Interface Sci.* **2001**, *94*, 53−81.
(29) Bates, F. S.; Fredrickson, G. H. *Annu. Rev. Phys. Chem.* **1990**, *41*, 525−557.
(30) Mansky, P.; Russell, T. P.; Hawker, C. J.; Mays, J.; Cook, D. C.; Satija, S. K. *Phys. Rev. Lett.* **1997**, *79*, 237−240.
(31) Amundson, K.; Helfand, E.; Quan, X.; Hudson, S. D.; Smith, S. D. *Macromolecules* **1994**, *27*, 6559−6570.
(32) Amundson, K.; Helfand, E.; Quan, X.; Smith, S. D. *Macromolecules* **1993**, *26*, 2698−2703.
(33) Thurn-Albrecht, T.; DeRouchey, J.; Russell, T. P.; Jaeger, H. M. *Macromolecules* **2000**, *33*, 3250−3253.
(34) Thurn-Albrecht, T.; Steiner, R.; DeRouchey, J.; Stafford, C. M.; Huang, E.; Bal, M.; Tuominen, M.; Hawker, C. J.; Russell, T. P. *Adv. Mater.* **2000**, *12*, 1138−1138.
(35) Russell, T. P.; Thurn-Albrecht, T.; Tuominen, M.; Huang, E.; Hawker, C. J. *Macromol. Symp.* **2000**, *159*, 77−88.
(36) Aoki, H.; Kunai, Y.; Ito, S.; Yamada, H.; Matsushige, K. *Appl. Surf. Sci.* **2002**, *188*, 534−538.
(37) Vavasour, J. D.; Whitmore, M. D. *Macromolecules* **2001**, *34*, 3471−3483.
(38) Jeon, H. G.; Hudson, S. D.; Ishida, H.; Smith, S. D. *Macromolecules* **1999**, *32*, 1803−1808.
(39) Goldbach, J. T.; Russell, T. P.; Penelle, J. *Macromolecules* **2002**, *35*, 4271−4276.
(40) Hawker, C. J.; Elce, E.; Dao, J.; Volksen, W.; Russell, T. P.; Barclay, G. G. *Macromolecules* **1996**, *29*, 2686−2688.
(41) Bouas-Laurent, H.; Castellan, A.; Desvergne, J. P.; Lapouyade, R. *Chem. Soc. Rev.* **2001**, *30*, 248−263.
(42) Grimme, S.; Peyerimhoff, S. D.; Bouas-Laurent, H.; Desvergne, J.-P. *Phys. Chem. Chem. Phys.* **1999**, *1*, 2457−2462.
(43) Bouas-Laurent, H.; Castellan, A.; Desvergne, J.-P. *Pure Appl. Chem.* **1980**, *52*, 2633−2648.
(44) Bouas-Laurent, H.; Castellan, A.; Desvergne, J. P.; Lapouyade, R. *Chem. Soc. Rev.* **2000**, *29*, 43−55.
(45) Condo, P. D.; Johnston, K. P. *J. Polym. Sci., Part B: Polym. Phys.* **1994**, *32*, 523−533.
(46) Condo, P. D.; Paul, D. R.; Johnston, K. P. *Macromolecules* **1994**, *27*, 365−371.
(47) Sato, Y.; Yurugi, M.; Fujiwara, K.; Takishima, S.; Masuoka, H. *Fluid Phase Equilib.* **1996**, *125*, 129−138.
(48) Wissinger, R. G.; Paulaitis, M. E. *J. Polym. Sci., Part B: Polym. Phys.* **1987**, *25*, 2497−2510.
(49) Ramachandrarao, V. S.; Gupta, R. R.; Russell, T. P.; Watkins, J. J. *Macromolecules* **2001**, 7923−7925.
(50) Shin, K.; Leach, A.; Goldbach, J. T.; Kim, D. H.; Jho, J. Y.; Tuominen, M. T.; Hawker, C. J.; Russell, T. P. *Nano Lett.* **2002**, *2*, 933−936.
(51) Kim, H. C.; Russell, T. P. *J. Polym. Sci., Part B: Polym. Phys.* **2001**, *39*, 663−668.

MA0489117